250
1-27-77
UC-79d Plus
UK-Germany-Japan

MASTER

Dr 651

HEDL-TME 76-87
UC-79,d

ANALYSIS OF SMALL-SAMPLE REACTIVITY WORTHS IN THE FAST TEST REACTOR ENGINEERING MOCKUP CRITICAL

HANFORD ENGINEERING DEVELOPMENT LABORATORY
Operated by Westinghouse Hanford Company
A Subsidiary of Westinghouse Electric Corporation

P.O. Box 1970 Richland, WA 99352

Prepared for the U.S. Energy Research and Development Administration under Contract No. EY-76-C-14-2170

NOTICE

Printed in the United States of America
Available from
National Technical Information Service
U.S. Department of Commerce
5285 Port Royal Road
Springfield, Virginia 22161
Price: Printed Copy $ 4.00 ; Microfiche $2.25

HEDL-TME 76-87
UC-79,d

ANALYSIS OF SMALL-SAMPLE REACTIVITY WORTHS IN THE FAST TEST REACTOR ENGINEERING MOCKUP CRITICAL

K. D. Dobbin and J. W. Daughtry

December 1976

Hanford Engineering Development Laboratory

Operated by the **Westinghouse Hanford Company** | A Subsidiary of Westinghouse Electric Corporation | for the United States Energy Research and Development Administration Contract No EY-76-C-14-2170

HEDL-TME 76-87
UC-79,d

ANALYSIS OF SMALL-SAMPLE REACTIVITY WORTHS IN THE FAST TEST REACTOR ENGINEERING MOCKUP CRITICAL

K. D. Dobbin and J. W. Daughtry

ABSTRACT

Small-sample reactivity worths were computed and compared with measurements at core center and along a radial traverse of the Fast Test Reactor Engineering Mockup Critical (FTR-EMC). The computed worths were obtained with first order perturbation theory using real and adjoint neutron fluxes from 42-group X-Y diffusion theory calculations. The perturbation demoninator (importance-weighted neutron production rate) was obtained from three-dimensional X-Y-Z calculations. For most of the calculated worths, cross sections were from the FTR Set 300S library (essentially ENDF/B version III data); however, ENDF/B version IV delayed neutron parameters were used to generate the necessary conversion factor to allow comparison of measured and calculated worths. At core center the C/E values were 1.14 to 1.33 for plutonium samples, 1.11 for a depleted uranium sample, 0.97 to 1.05 for boron, 0.89 to 1.08 for europia, 1.4 for stainless steel and 2.6 for iron oxide.

CONTENTS

FIGURES

TABLES

ANALYSIS OF SMALL-SAMPLE REACTIVITY WORTHS IN THE FAST TEST REACTOR ENGINEERING MOCKUP CRITICAL

1.0 INTRODUCTION

Previous Fast Test Reactor Engineering Mockup Critical (FTR-EMC) experiment analyses have examined the reactivity worths of moving or replacing FTR subassembly size material masses. Those studies included:

1. Fuel motion at the core center,[1]
2. Material substitution in the test loops,[2]
3. Substitution of high ^{240}Pu fuel for initial FTR fuel,[3]
4. B_4C safety rod (SR) and control rod (CR) motion,[4,5]
5. B_4C peripheral shim rod (PSR) removal,[4,5] and
6. Europium control rod removal.[5]

Reactivity worths for these material changes were computed by eigenvalue difference methods. Calculation-to-experiment bias factors were determined for use in FTR neutronics work.

Additional experiments, reported herein, were performed in the FTR-EMC to measure the worth of small samples of important FTR materials. The analysis of these small sample worth experiments is the subject of this report. Ten sample worths were measured at the core center. Included were four samples containing plutonium, two boron, a depleted uranium, a stainless steel, an iron oxide, and one sample containing europium oxide. These measurements provided information which can be used to evaluate current analytical methods and cross sections. Radial traverse measurements were made for three of the plutonium samples containing primarily ^{239}Pu, ^{240}Pu, and ^{241}Pu, respectively. These data were obtained to investigate changes in material worths near core heterogeneities.

In this analysis the computed sample worths were compared with measurements in order to assess the ability of present calculational tools to predict these worths. Calculation-to-experiment bias factors were obtained which can be used to adjust calculations of small perturbations in the FTR.

This report briefly describes the experiment, explains in detail the analytical methods, presents the measured and calculated results, compares these results, and tabulates the bias factors obtained.

2.0 SUMMARY

An experiment was performed in the FTR-EMC at Argonne National Laboratory to measure the reactivity worths of small samples. Worths of ten samples containing important FTR core materials were measured at core center and the worths of three of the samples containing plutonium were measured along a radial traverse.

Reactivity worths for each of the isotopes or elements in the samples were computed with first order perturbation theory using real and adjoint neutron fluxes from 42-group X-Y diffusion theory calculations. The perturbation denominator (importance-weighted neutron production rate) was obtained from three-dimensional X-Y-Z calculations. For most of the calculated worths the cross sections were from the FTR Set 300S library[6] (essentially ENDF/B version III data); however, ENDF/B version IV delayed neutron parameters[7] were used to generate the necessary conversion factor (980.2 Ih/%(Δk/k))[8] to allow comparison of measured and calculated worths. Sample worths were determined by combining the isotopic or elemental worths according to the mass of each in the sample. At core center the C/E values were 1.14 to 1.33 for plutonium samples, 1.11 for a depleted uranium sample, 0.97 for enriched boron, 1.04 for natural boron, 0.89 for europia using ENDF/B version III data, 1.08 for europia using version IV data, 1.4 for stainless steel, and 2.6 for iron oxide.

Along the radial traverse, C/E values varied as a function of radial position and proximity to heterogeneities.

3.0 EXPERIMENT

The FTR-EMC was assembled in the ZPR-9 critical facility at Argonne National Laboratory (ANL). Reference 9 presents a complete description of the EMC. The program of experiments performed in the EMC was divided into two phases. The first phase, designated Phase C of the FFTF critical experiments program,[10] was composed of experiments related to core and shielding design and to safety considerations having direct impact on the design. The second phase of experiments, designated Phase D, consisted of measurements related to FFTF operations and safety.

Measurements of the small-sample worths constituted Part VII of Phase D. The purpose of this experiment was to determine the worth of samples containing important FTR materials near core center and along a radial traverse.

3.1 Core Reference Configuration

The reference configuration for the small-sample worth experiment[11,12] was designated BOL-REF-5S, and simulated the FTR at the beginning-of-life. Figure 1 is a diagram of the BOL-REF-5S configuration viewed at the midplane of the assembly with modifications made to measure the worths of the small samples. A sample traverse hole extended radially along matrix row 23 from core center to the edge of the assembly. The hole was approximately 2.86 cm in diameter and was located in the stationary half about 4.45 cm in the axial direction from the core midplane. A calibrated autorod replaced outer driver material in matrix tube 23-14.* To compensate for the reactivity loss of these loading changes, the outer core-radial reflector boundary was changed by replacing radial reflector with outer driver composition in matrix tubes 22-12, 13-30, and 14-30. These modifications are identified on Figure 1.

---

*Matrix positions are identified by row number and column number in that order. See Figure 1.

ID	INNER DRIVER	SR	SAFETY ROD
OD	OUTER DRIVER	CR	CONTROL ROD
GP	GENERAL PURPOSE LOOP	PSR	PERIPHERAL SHIM ROD
SP	SPECIAL PURPOSE LOOP	X	AUTOROD
MT	MATERIAL TEST	A	REACTIVITY ADJUSTMENT TUBES

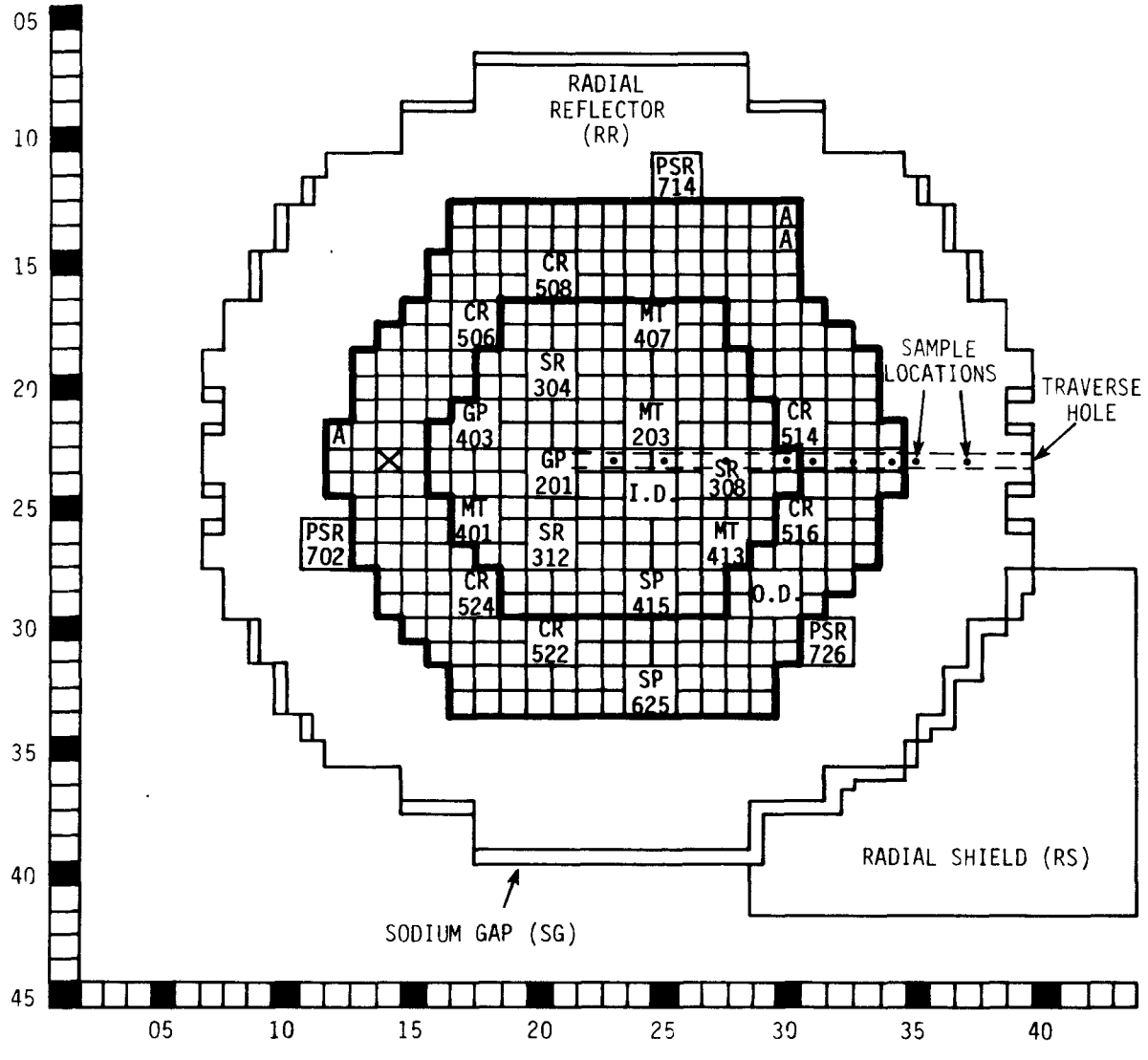

HEDL 7607-34.4

FIGURE 1. BOL-REF-5S Core Configuration.

Figure 2 illustrates the axial detail of each of the regions identified in Figure 1. For the small-sample worth experiment, control rods 508, 516 and 524 were inserted while control rods 506, 514, and 522, plus safety rods 304, 308, and 312 were parked.*

3.2 Experimental Procedure

The reactivity worth of a sample was measured by pneumatically injecting it into and out of the core, while the calibrated autorod maintained a constant power level. From the difference in average position of the autorod between the sample-in and sample-out cases, the reactivity effect was determined. Samples could be stopped at any location along the traverse so that the sample worth could be determined at the core center and along the radial traverse. Since samples were transported in sample capsules and capsule holders, the reactivity worth of the transport mechanism was also measured excluding the sample. From the two sets of data, worth of the sample alone was determined.

The reactivity worths of nine samples and a stainless steel capsule were measured at core center while only three samples, containing various plutonium isotopic compositions, were measured along the traverse tube. Table I lists the elemental and isotopic compositions of each sample. Reference 11 describes the experiment and experimental procedure in more detail.

Measured worths of the samples are tabulated in Section 5. A conversion factor of 980.2 Ih/%(Δk/k) was used to convert the reactivity worths reported in inhours to units of Δk/k for comparison with calculations. Previous EMC analyses have used 1047.7 Ih/%(Δk/k), a value computed by ANL using Keepin's[13] delayed neutron data. ENDF/B version IV contains delayed neutron parameters based on an evaluation which included the Keepin data as well as the results of more recent measurements. Using these parameters, a conversion factor of 980.2 Ih/%(Δk/k) was obtained.[8]

*A control rod is parked when it is withdrawn 36 inches from a full inserted position with the original control rod location filled with sodium channel composition. The parked rod position is shown as SR, CR (OUT) in Figure 2.

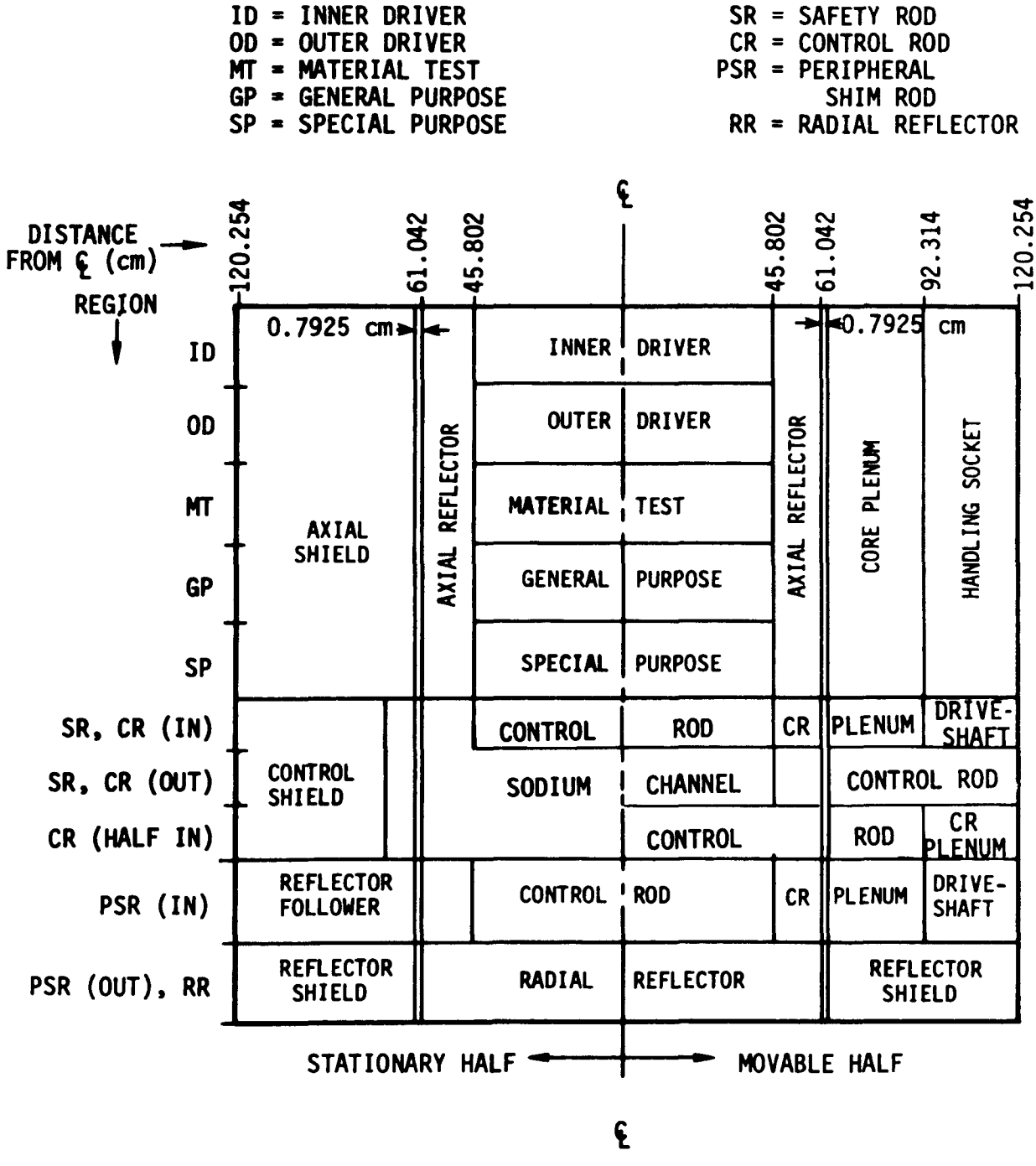

FIGURE 2. Axial Detail of EMC Core.

TABLE I

SAMPLE COMPOSITIONS

Sample Identification	Constituent Materials	Mass (wt.%)
MB-11	^{239}Pu	96.9380
	^{240}Pu	0.9919
	^{241}Pu	0.0517
	^{242}Pu	0.0033
	Al	1.2075
Pu-R	^{239}Pu	0.904
	^{240}Pu	80.70
	^{241}Pu	0.49
	^{242}Pu	4.00
	O	11.97
	H	0.035
	N	0.02
Pu-50	^{239}Pu	1.005
	^{240}Pu	2.688
	^{241}Pu	65.429
	^{242}Pu	1.348
	Am	16.38
	O	12.05
Pu-242-4-1	^{239}Pu	1.48
	^{240}Pu	0.0925
	^{241}Pu	0.0069
	^{242}Pu	98.22
MB-25	^{235}U	0.2328
	^{238}U	99.7672
B-7	^{10}B	87.12
	^{11}B	7.38
	Si	0.26
	Al	0.05
	O	1.43
	H	0.09
	C	0.96
B(L)	^{10}B	19.88
	^{11}B	80.12
304 SS	Fe	70.4
	Cr	18.4
	Ni	9.7
	Mn	1.5

4.0 ANALYTICAL METHODS

First order perturbation theory (FOP) was used to compute the reactivity worths of all the elements and isotopes in the small samples described in Section 3.2. Two-dimensional (2-D) X-Y perturbation calculations were used with a perturbation denominator normalized to three-dimensional (3-D) results obtained from a 12-neutron energy group, 2 x 2-inch X-Y mesh model. The normalization factor was established by comparison with a 2-D model using both the 30-group structure from which the 12 groups were collapsed and the 3-D 2 x 2-inch X-Y mesh. Reactivity worths were calculated in a 42-group model using a 1 x 1-inch X-Y mesh along the traverse where heterogeneities produced significant flux gradients. Sections 4.2 and 4.3 describe these models and the computational procedures in detail.

4.1 Neutron Cross Section Preparation

Neutron cross sections used in this analysis are from the 30-neutron energy group FTR Set 300[14] and the 42-group FTR Set 300S[6] libraries. Both libraries were generated with the ETOX[15] program from ENDF/B version II data modified so that they are nearly equivalent to ENDF/B version III data. For those materials that are common to both libraries, the cross sections in the first 25 groups are identical. Set 300S, with its greater low-energy resolution, was developed primarily for shielding calculations.

Two types of cross sections were needed. Reactor flux calculations required appropriate cross sections for all reactor materials. Reference 16 describes the preparation of these cross sections in 30 and 42 groups for materials near the core midplane. These cross sections were used in the 2-D calculations. The 30-group set was collapsed to 12 groups and cross sections for the axial regions of the EMC were added in an earlier study.[1] The resulting combined 12-group set was used in the 3-D calculations. Figure 3 illustrates the group structure of the cross section sets.

Small-sample cross sections were prepared in 42 groups. For the small samples at the core center, all the materials were homogeneously resonance self-shielded for an inner core position except Eu and ^{242}Pu which were treated as infinitely dilute. Along the traverse the resonance

LETHARGY WIDTH	42 GROUP	30 GROUP	12 GROUP
0.5	1	1	1
0.5	2	2	
0.5	3	3	2
0.5	4	4	
0.5	5	5	3
0.5	6	6	
0.25	7	7	4
0.25	8	8	
0.5	9	9	5
0.5	10	10	
0.5	11	11	6
0.5	12	12	
0.47	13	13	7
0.25	14	14	
0.28	15	15	
0.5	16	16	8
0.5	17	17	
0.5	18	18	9
0.167	19	19	
0.167	20	20	
0.167	21	21	
0.5	22	22	10
0.5	23	23	
0.5	24	24	11
0.5	25	25	
0.5	26	26	12
0.5	27		
0.5	28	27	
0.5	29	28	
0.5	30		
0.5	31		
0.5	32	29	
0.5	33		
0.5	34		
0.5	35		
0.5	36		
0.5	37		
0.5	38	30	
0.5	39		
0.5	40		
0.5	41		
	42		

HEDL 7510-229.1

FIGURE 3. Group Structure of Cross Section Sets.

self-shielding was performed in inner driver material over the inner driver section and outer driver material over the outer driver section. In the radial reflector all sample cross sections were infinitely dilute.

4.2 Three-Dimensional Model

A three-dimensional model was used to improve the accuracy of the computed perturbation denominator. Modifications were made to the model described in reference 4 to establish the loading pattern shown in Figure 1. Mesh spacing in the X and Y directions of approximately 5.53 cm was equivalent to the dimensions of the ZPR-9 matrix tubes. The energy boundaries of the twelve energy group cross section set used in this analysis were the same as those used in previous EMC analyses[1,2] (see Figure 3).

Real and adjoint fluxes were computed using the 3-D neutron diffusion theory program, 3DB.[17] These fluxes were input to the 3-D perturbation theory program, 3DP,[18] to compute the perturbation denominator. Also, reactivity worths were computed at core center for the plutonium and uranium isotopes using core cross sections. These worths were used only for comparing 2-D and 3-D perturbation denominators. Section 5.2 presents these results.

4.3 Two-Dimensional Model

Two 2-D models were developed in this study. One was a comparison 2-D model to establish a volume factor to adjust the 2-D perturbation denominator. Thirty neutron energy groups were selected to be consistent with the library from which the 12-group set used in the 3-D calculations was collapsed. This model used an X-Y mesh spacing of 5.53 cm in each direction which was equivalent to the 3-D spacing. A space and energy independent axial buckling of 0.000565 cm^{-2} was used for all the calculations to account for neutron leakage in the Z direction. This value was derived in a previous study[19] from a comparison of a single set of 3-D X-Y-Z and 2-D X-Y calculations. Atom densities were taken from reference 9 and adjusted for ^{241}Pu decay to the date of the experiment. The total real neutron flux was normalized to the 3-D flux at matrix location 23-23.

From the ratio of the perturbation denominator (PD) calculated by the 3-D model to that of the 2-D model, a volume factor was established to adjust the PD of all subsequent 2-D calculations. Reactivity worths were computed at the core center using core cross sections, for convenience, to compare with the 3-D results. These worth computations were performed only as a 3-D-to-2-D comparison where any errors caused by using a heterogeneous geometry in the cross section preparation would cancel.

To be consistent between the computed reactivity worths at the core center and along the radial traverse, one 2-D model was used for all sample worth computations. Better low-energy resolution was obtained by using the 42-group structure mentioned previously which divided groups 26 to 30 of the 30-group set into 17 groups. Previous studies[2] have concluded that this energy resolution is important to accurately predict fission rates in and near the reflector.

Because of the heterogeneities in the EMC along the sample worth traverse, a finer neutron flux mesh structure was selected. The 2-inch mesh was changed to 1 inch between matrix tube rows 13 and 25 and columns 26 to 37 inclusive. Therefore, the center sample and the one adjacent were located where the mesh was 2 inches wide along the traverse and 1 inch perpendicular. The rest of the samples were located where the mesh spacing was 1 inch by 1 inch.

Real and adjoint fluxes were computed using this fine-group and fine-mesh model and the 2-D neutron diffusion theory program, 2DBS.[20] These fluxes, along with the appropriate cross sections described in Section 4.1, were input to the 2-D perturbation theory program, PERT-V.[21] A volume factor was added from the 3-D-to-2-D comparison to adjust the perturbation denominator. Reactivity worths were computed at matrix location 23-23 for the constituents of all the samples measured at the core center. The constituent worths were combined according to their weight fractions to form the sample worths. For the plutonium sample traverses, the constituent isotope and element worths were computed for every flux mesh point along the traverse. Lagrangian interpolation was used to discreetly determine the computed worth over the length of each sample. The worth of each constituent

was numerically integrated over the sample length and combined according to its weight fraction with other constituents to determine the sample worths at each sample location. Section 5.2 presents the computed results.

5.0 RESULTS AND COMPARISONS WITH EXPERIMENT

5.1 Experimental Results

Table II presents the reactivity worths of the samples measured at the core center. These data, reported by ANL in units of inhours, were converted to ($\Delta k/k$) using the factor 980.2 Ih/%($\Delta k/k$) as discussed in Section 3.2. Table III lists the worths of the samples measured radially along the sample traverse hole. These samples are identified by their position compared with the central sample located in matrix tube 23-23. Notice that Table III assigns the sample positions both by the distance in centimeters and the number of matrix tubes or drawers. The latter unit of measurement is selected to easier identify the sample locations which were selected at the center or boundary of drawer columns. Plots of these data are included in Section 5.2 along with the computed results.

5.2 Analytical Results

Results of the 3-D to 2-D comparison calculations included a volume factor to adjust the 2-D computed perturbation denominator. This factor of 63.20, which was used for this study, was obtained from the ratio of the PD computed by the 3-D 12-group model to that computed by the 2-D 30-group model. However, the volume factor could also be obtained from adjusting central 2-D computed worths to be equal to the central 3-D worths. Table IV gives the 3-D and 2-D computed worths and the ratios of those worths for several important FTR fuel isotopes. The deviation of the worth ratios from the ratio of perturbation denominators is less than 1 percent for all four isotopes.

The 2-D, X-Y 42-group fine mesh model described in Section 4.3 was used for all the subsequent reactivity worth calculations. Table V lists the computed reactivity worths of the elements and isotopes of the experiment samples at the core center.

Central sample reactivity worths were computed from the constituent worths in Table V by combining them according to their weight contributions.

TABLE II

MEASURED CENTRAL SAMPLE REACTIVITY WORTHS

Sample ID	Principal Constituents	Sample Mass(g)	Sample Length (cm)	Sample Worth[(a)] (Δk/k per kg)
MB-11	^{239}Pu	21.409	3.18	0.0024644 ± 0.0000028
Pu-R	^{240}Pu	13.776	4.78	0.0002355 ± 0.0000037
Pu-50	^{241}Pu	0.5817	0.399	0.002408 ± 0.000099
Pu-242	^{242}Pu	27.295	2.07	0.0002544 ± 0.0000031
MB-25	^{238}U	38.163	4.2863	-0.0001545 ± 0.0000014
304 SS	Fe	154.205	5.08	-0.00005892± 0.00000038
	Cr			
	Ni			
	Mn			
Fe_2O_3-2	Fe	5.2648	5.509	-0.0000352± 0.0000113
	O			
B-7	^{10}B	0.4968	5.519	-0.04598 ± 0.00012
	^{11}B			
B(L)	^{10}B	0.5553	5.519	-0.009896 ± 0.000089
	^{11}B			
Eu_2O_3	Eu-151	9.9634	5.494	-0.003269 ± 0.000005
	Eu-153			

(a) Conversion factor = 980.2 Ih/%(Δk/k).

TABLE III

MEASURED WORTHS OF SELECTED PLUTONIUM SAMPLES

Radial Distance from Center		Sample Worths (Δk/k per kg)[a]		
cm	Number of Drawers	MB-11[b]	Pu-R[b]	Pu-50[b]
0.0	0	0.002464 ± 0.000003	0.000236 ± 0.000004	0.00241 ± 0.00010
11.06	2	0.002372 ± 0.000003	0.000202 ± 0.000002	0.00222 ± 0.00009
24.89	4.5	0.001930 ± 0.000004	0.000174 ± 0.000002	0.00182 ± 0.00010
38.71	7	0.001405 ± 0.000003	0.000162 ± 0.000004	0.00132 ± 0.00009
44.25	8	0.001195 ± 0.000002	0.000147 ± 0.000003	0.00119 ± 0.00009
52.55	9.5	0.000784 ± 0.000002	0.000112 ± 0.000003	0.00072 ± 0.00010
60.83	11	0.000562 ± 0.000002	0.000061 ± 0.000004	0.00060 ± 0.00009
66.37	12	0.000463 ± 0.000003	0.000031 ± 0.000004	0.00069 ± 0.00014
77.44	14	0.000204 ± 0.000003	0.000017 ± 0.000004	0.00030 ± 0.00021

(a) Conversion factor = 980.2 Ih/%(Δk/k).

(b) See Table I for sample compositions.

TABLE IV

COMPARISON OF 3D-2D NORMALIZATIONS

	Worth, $\Delta\rho$ ($\Delta k/k$) per kg			
Material	3D[a]	2D[b]	$\Delta\rho_{2D}/\Delta\rho_{3D}$	% Difference[c]
Pu-239	0.002914	0.1840	63.14	+0.09
Pu-240	0.0003972	0.02496	62.84	+0.57
Pu-241	0.004129	0.2607	63.14	+0.09
U-238	-0.0001636	-0.01040	63.57	-0.59

(a) From 12-group, 2" x 2" 3-D calculation.

(b) From 30-group, 2" x 2" 2-D calculation.

(c) % difference = $\dfrac{\left(\dfrac{PD_{3D}}{PD_{2D}} - \dfrac{\Delta\rho_{2D}}{\Delta\rho_{3D}}\right)}{\left(\dfrac{PD_{3D}}{PD_{2D}}\right)} \times 100$

where: $\dfrac{PD_{3D}}{PD_{2D}} = 63.20$ = volume factor

TABLE V

COMPUTED CENTRAL SAMPLE CONSTITUENT WORTHS

Element or Isotope	Worth ($\Delta k/k$ per kg)
Pu-239	0.002886
Pu-240	0.0003398
Pu-241	0.004144
Pu-242	0.0002502
U-235	0.002227
U-238	-0.0001774
O-16	-0.0001378
Al	-0.0001168
Fe	-0.00007052
Cr	-0.00009280
Ni	-0.0001147
Mn	-0.0002530
Mo	-0.0003308
B-10	-0.051285
B-11	-0.0001816
Eu-151	-0.003893
Eu-153	-0.002871
Eu-151[a]	-0.004791
Eu-153[a]	-0.002996

(a) Computed with ENDF/B Version IV cross section data.

The results are listed in Table VI along with the C/E biases. Uncertainties in the C/E values reflect only the uncertainty in the experiment. The uncertainty in the C/E due to uncertainties in the computations is included in the C/E itself.

For the plutonium and boron samples, an equal number of samples containing different isotopic compositions were measured as there were unknown isotopic worths to be determined (^{241}Am, ^{16}O, and Al were assumed to have a negligible net reactivity worth at core center). Simultaneous equations involving the weight fraction and worth of each isotope and the total measured sample worth of each of the four plutonium and two boron samples were solved for the isotopic worths. Table VII tabulates the resulting inferred isotopic worths and C/E bias factors.

The reactivity worths of the elemental and isotopic constituents of the radial worth traverse samples were computed at every flux mesh point along the traverse. An average was reported for two mesh points in the direction along the axis perpendicular to the traverse. Table VIII lists these worths normalized to a 1 kg sample and Figures 4 to 9 plot the computed worth profiles of each. A drawing of the portion of the EMC core where the samples were located is included at the top of each figure for quick reference. The radial position along the traverse is plotted in units of EMC drawers which are approximately 5.53 cm along their edges in the X and Y directions.

Using the data handling scheme described in Section 4.3, the worth of each of the samples was determined by integrating each of the worth curves over the sample lengths. Table IX lists these computed results. The uncertainty given for the C/E biases includes only the reported uncertainty in the experimental measurements. Resulting radial worth profiles are plotted in Figures 10 to 12.

TABLE VI

COMPUTED CENTRAL SAMPLE WORTHS

Sample ID[a]	Sample Worth ($\Delta k/k$ per kg)	C/E
MB-11	0.002802	1.137 ± 0.001[b]
Pu-R	0.0003142	1.334 ± 0.021
Pu-50	0.002736	1.136 ± 0.047
Pu-242	0.0002890	1.136 ± 0.014
MB-25	-0.0001718	1.112 ± 0.010
304 SS	-0.00008164	1.386 ± 0.009
Fe_2O_3-2	-0.00009074	2.58 ± 0.83
B-7	-0.044695	0.972 ± 0.003
B(L)	-0.010341	1.045 ± 0.009
Eu_2O_3-3	-0.002920	0.893 ± 0.001
Eu_2O_3-3-IV[c]	-0.003516	1.075 ± 0.002

(a) See Table I for sample compositions.

(b) Quoted uncertainty in C/E is due to uncertainty in experiment only.

(c) Computed with ENDF/B Version IV cross section data.

TABLE VII

INFERRED CENTRAL SAMPLE ISOTOPIC WORTHS

Isotope	Worth ($\Delta k/k$ per kg)[a,b]	(C/E)[c]
Pu-239	0.002539 ± 0.0000028	1.136 ± 0.001[d]
Pu-240	0.0002308 ± 0.0000046	1.472 ± 0.029
Pu-241	0.003628 ± 0.0001512	1.143 ± 0.048
Pu-242	0.0002191 ± 0.0000031	1.142 ± 0.016
B-10	-0.05240 ± 0.00014	0.971 ± 0.003

(a) Inferred isotopic worths determined from the measured worths of four plutonium samples and two boron samples of differing isotopic compositions.

(b) Conversion factor = 980.2 Ih/%($\Delta k/k$).

(c) Calculated worths taken from Table V.

(d) Quoted uncertainty in C/E is due to uncertainty in experiment only.

TABLE VIII

COMPUTED RADIAL WORTH TRAVERSES FOR PLUTONIUM SAMPLE CONSTITUENTS

Distance From Center(cm)	Reactivity Worths (10^{-2} $\Delta k/k$ per Kg)					
	Pu-239	Pu-240	Pu-241	Pu-242	O-16	AL
0.0	0.2886	0.03398	0.4144	0.02502	-0.01378	-0.01168
5.53	0.2881	0.03038	0.4192	0.02158	-0.01317	-0.01114
11.06	0.2793	0.02867	0.4078	0.02016	-0.01233	-0.01051
15.21	0.2655	0.02809	0.3866	0.01992	-0.01032	-0.009245
17.98	0.2527	0.02611	0.3694	0.01825	-0.005865	-0.006347
20.74	0.2387	0.02271	0.3529	0.01524	-0.0002249	-0.002677
23.51	0.2285	0.02105	0.3390	0.01392	-0.0003244	-0.002602
26.27	0.2186	0.02033	0.3240	0.01352	-0.0007761	-0.002946
29.04	0.2093	0.02039	0.3086	0.01386	-0.003105	-0.003972
31.80	0.1986	0.02170	0.2888	0.01544	-0.006948	-0.006015
34.57	0.1842	0.02194	0.2653	0.01601	-0.006115	-0.005113
37.33	0.1700	0.02100	0.2438	0.01540	-0.005346	-0.004400
40.10	0.1568	0.01989	0.2242	0.01458	-0.004697	-0.003881
42.87	0.1440	0.01890	0.2054	0.01374	-0.003827	-0.003353
45.63	0.1316	0.01788	0.1869	0.01281	-0.002095	-0.002247
48.40	0.1183	0.01665	0.1675	0.01144	-0.001271	-0.001145
51.16	0.1046	0.01478	0.1486	0.009074	0.001558	0.000200
53.93	0.09093	0.01227	0.1309	0.005548	0.003845	0.001759
56.69	0.07765	0.00909	0.1152	0.0007405	0.006186	0.00340
59.46	0.06530	0.005108	0.1027	-0.005350	0.008320	0.004954
62.22	0.05476	-0.0001420	0.09554	-0.01230	0.010123	0.006351
64.99	0.06641	-0.02974	0.1261	-0.01525	0.008337	0.005625
67.75	0.08237	-0.01426	0.1532	-0.009223	0.004494	0.003481
70.52	0.08124	-0.007745	0.1474	-0.003827	0.002309	0.002164
73.29	0.06805	-0.002160	0.1216	-0.001137	0.001213	0.001376
76.05	0.05071	-0.0001690	0.08981	-0.000121	0.0007155	0.0009148
78.82	0.03430	0.0003330	0.06044	0.0001598	0.0005108	0.0006443
82.97	0.01566	0.0003256	0.02743	0.0001830	0.0004352	0.0004307

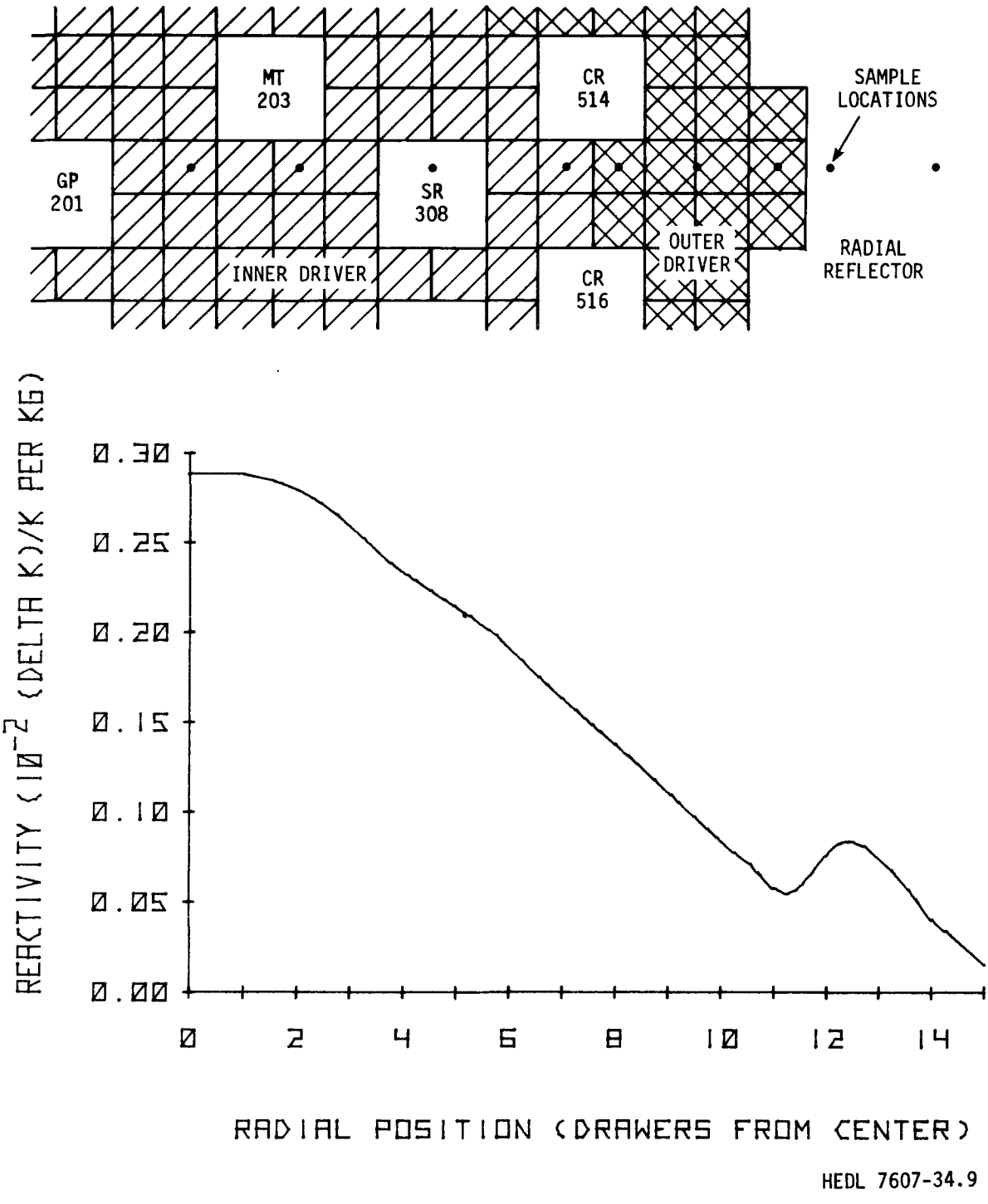

FIGURE 4. Computed Radial Worth Profile of ^{239}Pu.

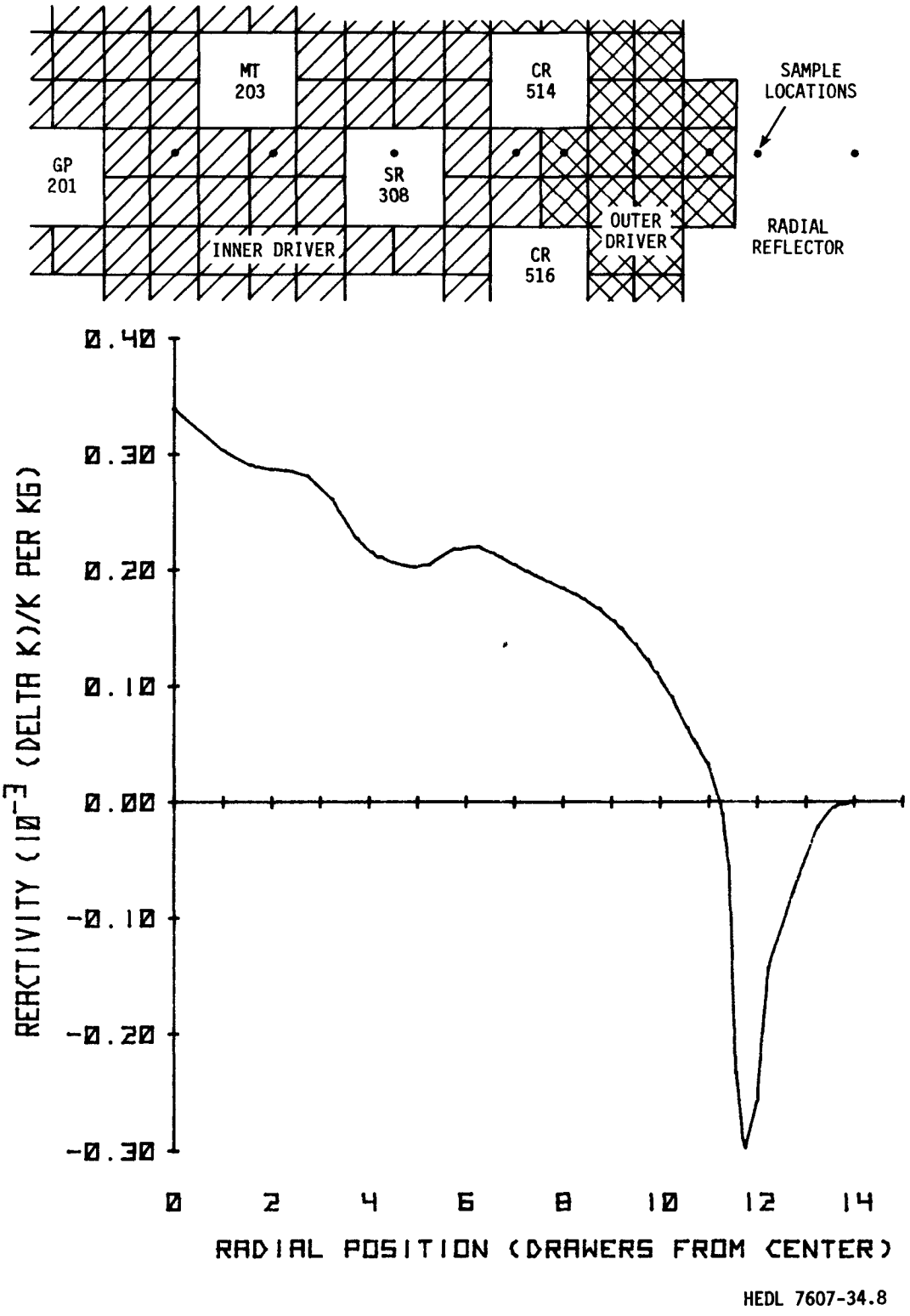

FIGURE 5. Computed Radial Worth Profile of ^{240}Pu.

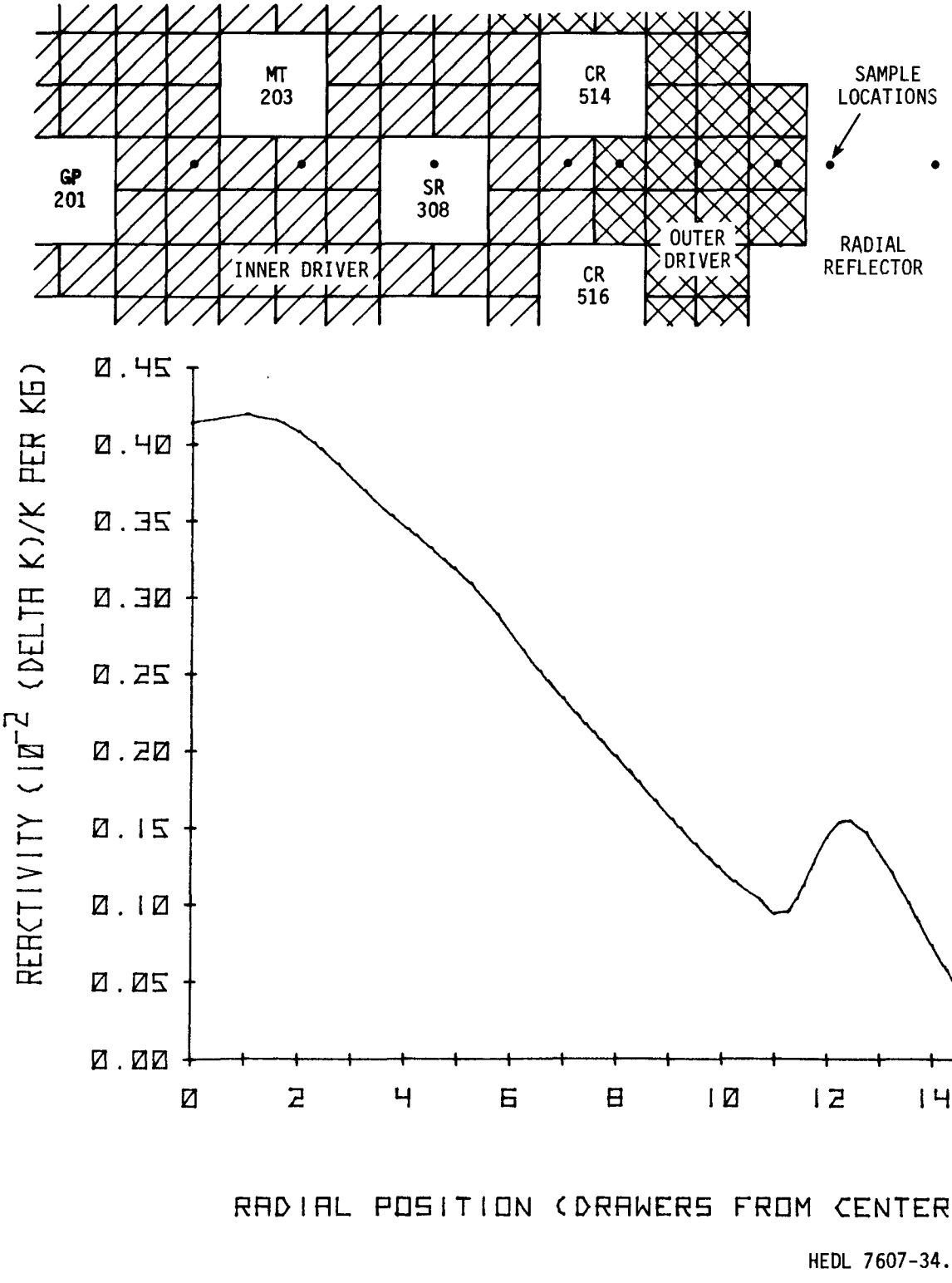

FIGURE 6. Computed Radial Worth Profile of ^{241}Pu.

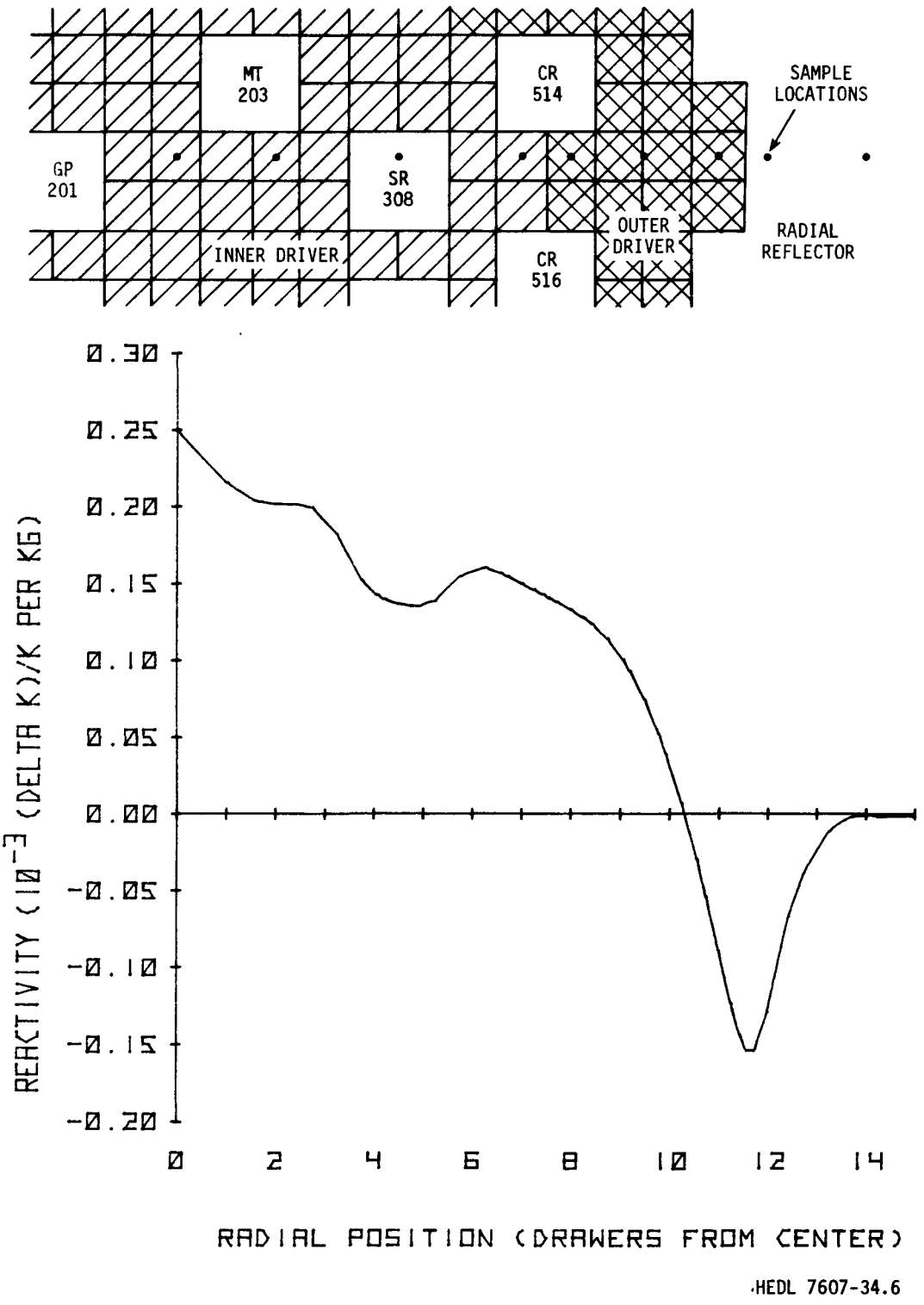

FIGURE 7. Computed Radial Worth Profile of ^{242}Pu.

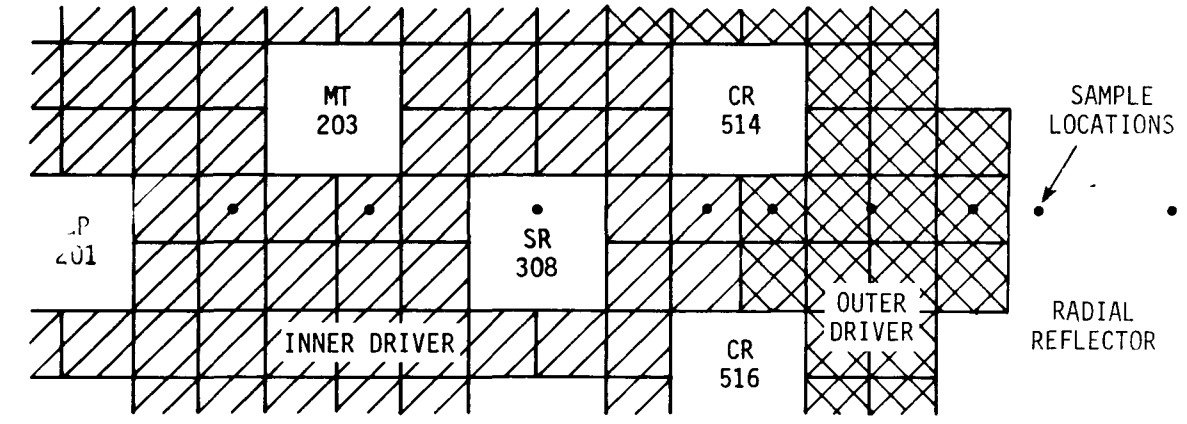

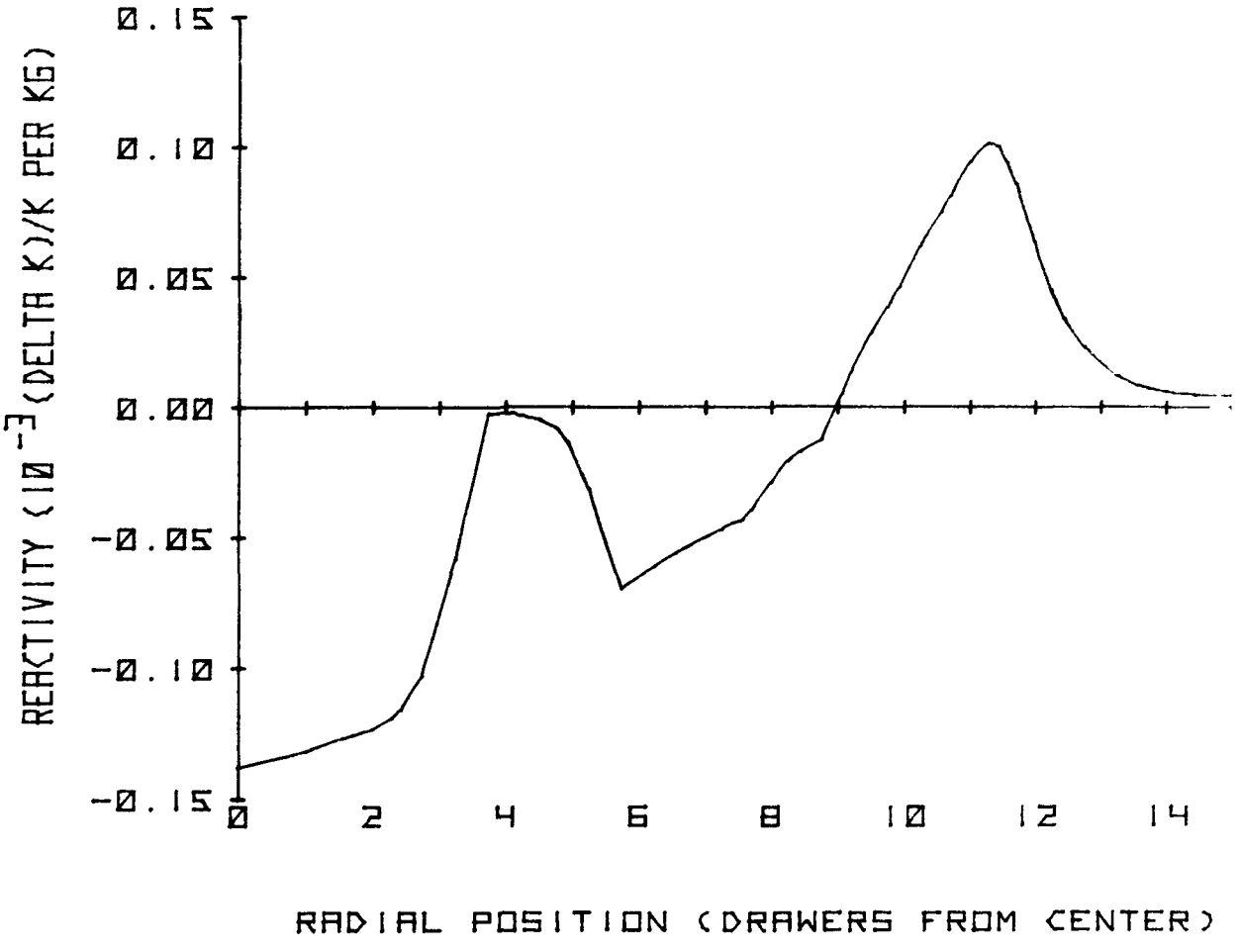

HEDL 7607-34.7

FIGURE 8. Computed Radial Worth Profile of ^{16}O.

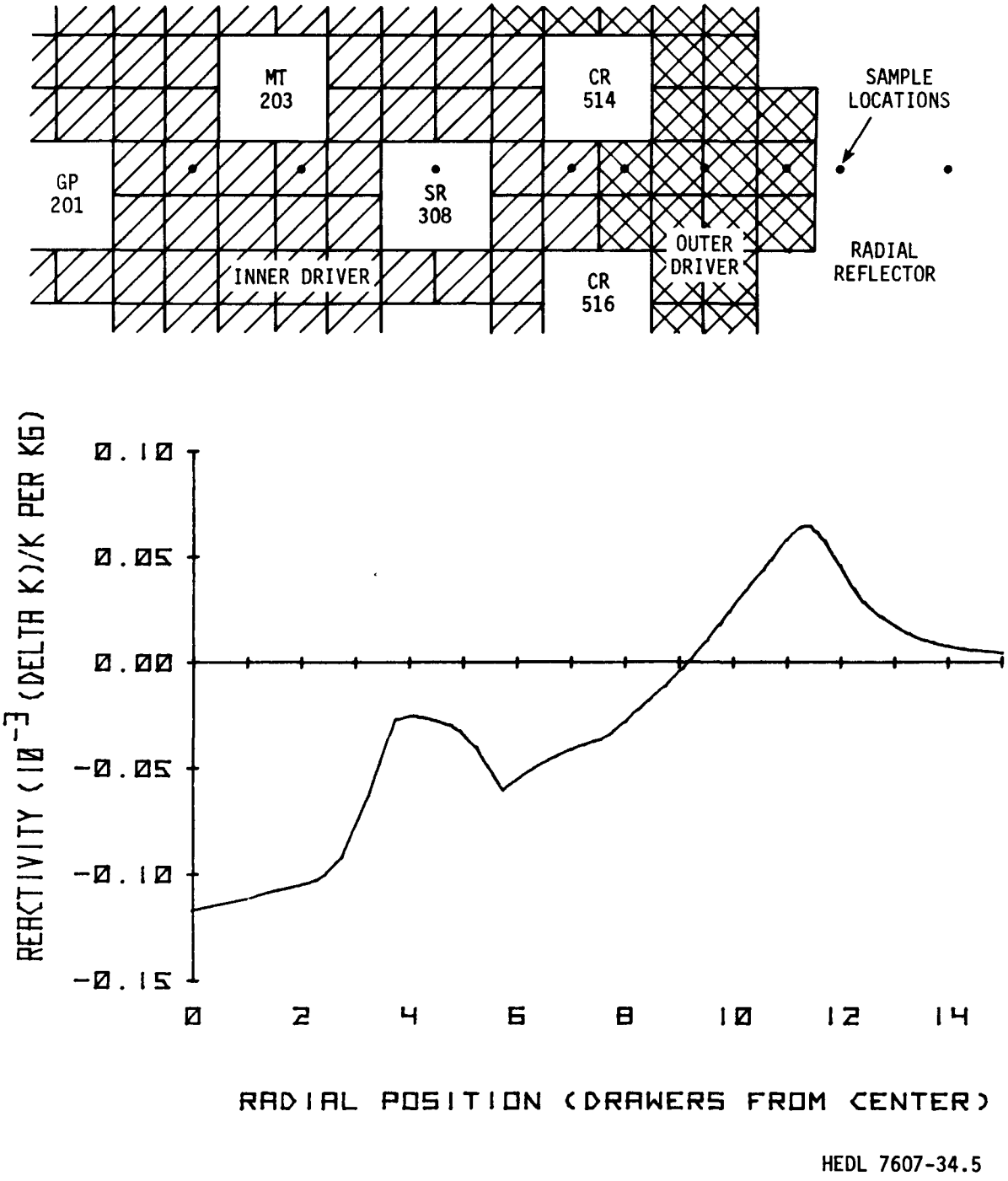

FIGURE 9. Computed Radial Worth Profile of Al.

TABLE IX

COMPUTED RADIAL WORTHS AND C/E BIASES FOR SELECTED PLUTONIUM SAMPLES

Radial Position from Center		MB-11 [a]		Pu-240-R [a]		Pu-50 [a]	
cm	No. of Drawers	Sample Worth (Δk/k)	C/E	Sample Worth (Δk/k)	C/E	Sample Worth (Δk/k)	C/E
0.0	0	0.002802	1.137±0.001 [b]	0.0003142	1.33±0.02	0.002736	1.14±0.05
11.06	2	0.002710	1.142±0.001	0.0002703	1.34±0.01	0.002692	1.21±0.05
24.89	4.5	0.002170	1.124±0.002	0.0002082	1.20±0.01	0.002199	1.21±0.07
38.71	7	0.001587	1.130±0.002	0.0001913	1.18±0.03	0.001548	1.17±0.08
44.25	8	0.001338	1.120±0.002	0.0001723	1.17±0.02	0.001301	1.09±0.08
52.55	9.5	0.0009491	1.211±0.003	0.0001246	1.11±0.03	0.0009306	1.3 ±0.2
60.83	11	0.0005712	1.016±0.004	0.00001476	0.24±0.02	0.0006345	1.1 ±0.2
66.37	12	0.0007324	1.58 ±0.01	-0.0001602	-5.2 ±0.7	0.0009436	1.4 ±0.3
77.44	14	0.0004026	1.97 ±0.03	0.000008911	0.52±0.12	0.0004891	1.6 ±1.1

(a) See Table I for sample compositions.

(b) Uncertainty in C/E due to uncertainty in experiment.

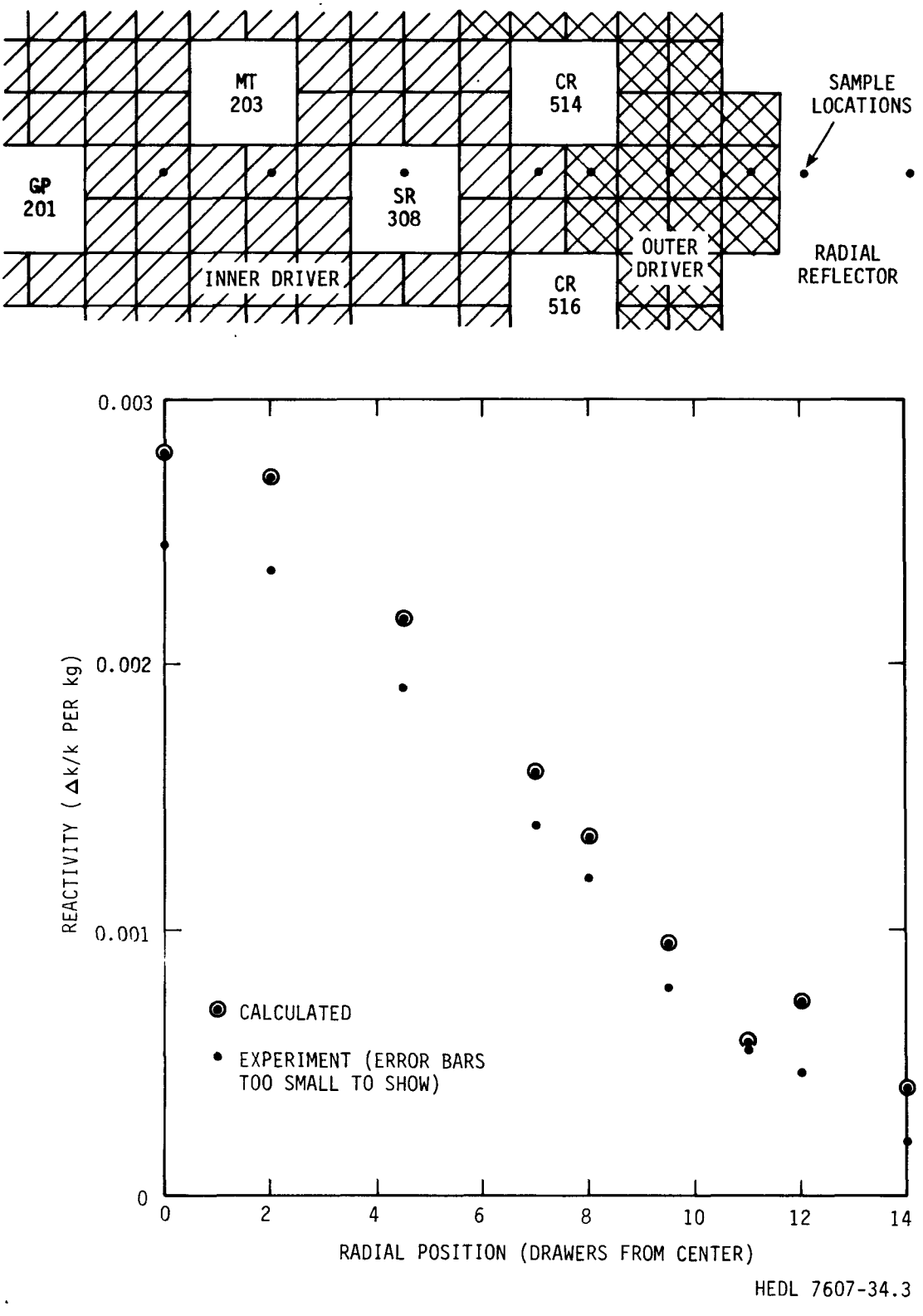

FIGURE 10. Radial Worth Profile of Sample MB-11, Containing Primarily ^{239}Pu.

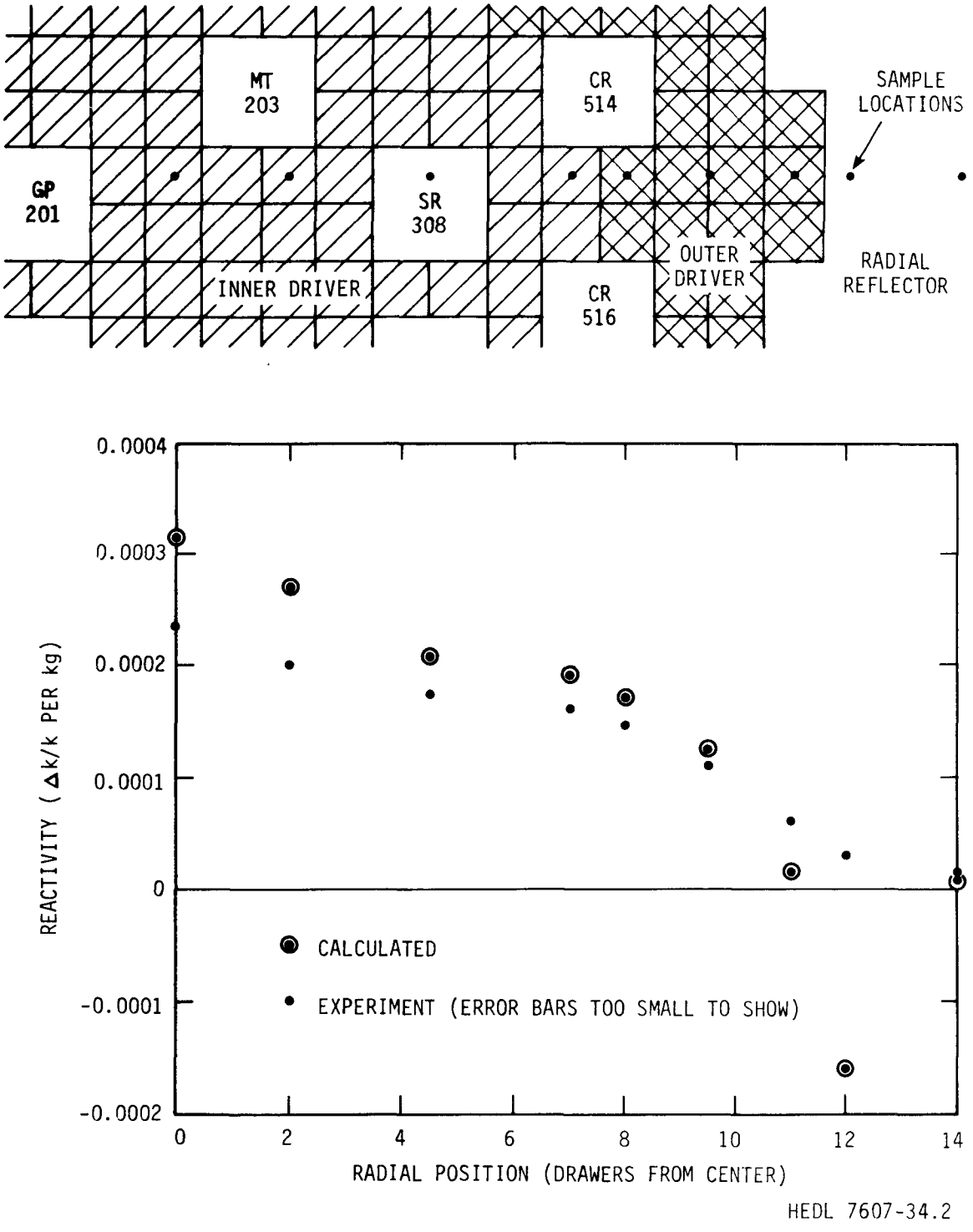

FIGURE 11. Radial Worth Profile of Sample Pu-R, Containing Primarily ^{240}Pu.

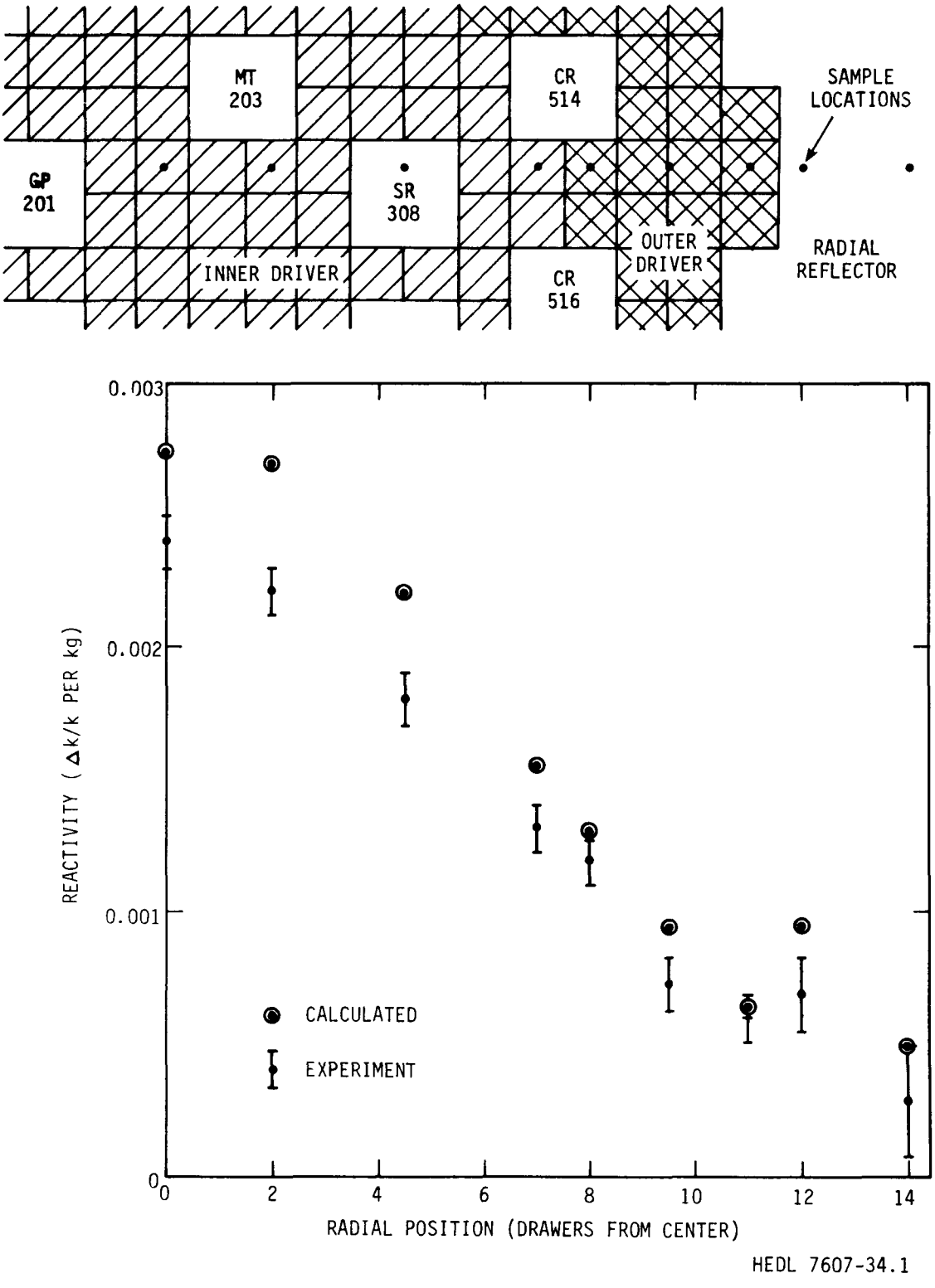

FIGURE 12. Radial Worth Profile of Sample Pu-50, Containing Primarily ^{241}Pu.

6.0 DISCUSSION AND CONCLUSIONS

Table V includes calculated worths of ^{151}Eu and ^{153}Eu using two different sets of cross section data. The first set of calculated results was obtained using cross sections from ENDF/B version III. The second set of worths was obtained using ENDF/B version IV cross sections. The version IV results are approximately 20 percent higher. A previous study[5] comparing B_4C and Eu_2O_3 control rod worths indicated that the version IV europium data are preferable. The version IV data yield C/E values a few percent closer to 1.0 in this study (see Table VI).

A comparison of calculated worths using version III and version IV cross section data for most of the other important isotopes in Table V has been published[22] elsewhere.

The C/E values for the central small-sample worths measured in the FTR-EMC are given in Table VI. It is of interest to compare these C/E values with those obtained in earlier analyses of FTR-related critical experiments. Small-sample worths were measured in the FTR-3 assembly[23] and computed[9] by Argonne National Laboratory (ANL) personnel using ENDF/B version I cross section data and by the Westinghouse Advanced Reactors Division (WARD) using modified[24] Bondarenko[25] cross section data. For a predominantly ^{239}Pu sample the C/E values were 1.26 (ANL) and 1.34 (WARD) compared to 1.14 in Table VI. For a depleted uranium sample the C/Es were 1.16 (ANL) and 1.12 (WARD) compared to 1.11 in Table VI. For an enriched boron sample the C/E values were 1.09* (ANL) and 0.99* (WARD) compared to 0.97 in Table VI. However, both earlier analyses used Keepin's[13] delayed neutron parameters. If the newer ENDF/B version IV evaluation (used in this report) had been used in the ANL and WARD analyses, all the earlier C/E values would have been reduced by about 7 percent.† Also, the effect of sample

* These are corrected values. The ANL and WARD reports contained incorrect boron sample compositions.

† Other evaluations of delayed neutron data could result in different C/E values. A more recent evaluation of reported delayed neutron data has been made by Tuttle.[26] An inhour-to-percent ($\Delta k/k$) conversion factor computed from this evaluation would produce C/E values lower than those based on ENDF/B version IV data, bringing the C/Es for fissile worth closer to 1.0 while at the same time taking the C/E for boron worth further below 1.0.

on the C/E values has not been taken into account in Table VI. Based on the results of previous studies[9,27] of size effects on sample worths, the C/E values in Table VI would become 1.17 for MB-11 (^{239}Pu), 0.97 for MB-25 (^{238}U) and 0.93 for B-7 (^{10}B). Taking all these effects into account, a comparison of results is given in Table X. Another factor that could alter the C/E values is the effect of the sample holder and traverse equipment on the sample worths. This effect has been estimated[9] to be of the order of a few percent and if included would change all of the results in Table X since this effect was not included in any of the analyses.

The isotopic worths and uncertainties in Table VII were derived from the sample worths and their uncertainties given in Table VI. The uncertainties in the isotopic worths are actually somewhat larger than indicated in Table VII because the contributions of ^{241}Am, oxygen and aluminum have been neglected and because sample size effects have not been taken into account.

TABLE X

COMPARISON OF C/E VALUES

Principal Isotope	WARD	ANL	This Report
^{239}Pu	1.27	1.19	1.17
^{238}U	1.05	1.09	0.97
^{10}B	0.92	1.02	0.93

Computed worth traverses for ^{239}Pu and ^{241}Pu are similar in shape (see Figures 4 and 6). The worths are maximum at the center, minimum just inside the core at the outer driver-radial reflector interface and peak in the reflector. For ^{240}Pu and ^{242}Pu (Figures 5 and 7), fission and absorption events compete. Fission dominates to produce a positive worth at the core center. Near the core edge the higher energy fission is reduced due to the softer spectrum allowing the negative worth of the absorption events to dominate. Near the assembly edge, the absorptions diminish and scattering events reduce radial neutron leakage, a positive worth effect. Heterogeneities along the traverse produce irregularities in the isotopic worth curves.

Notice the reduction in the positive worth of ^{240}Pu and ^{242}Pu inside the safety rod channel (SR 308) where the softer spectrum reduces the fast fission contribution.

For aluminum and ^{16}O (Figures 8 and 9), absorption and scattering events compete with absorption dominant inside the core. At the edge of the core, the worth of these materials is positive due to the reduction in the neutron leakage because of increased scattering.

Table VIII presents the computed radial worth traverses for the plutonium isotopes. Calculation-to-experiment comparisons could not be done off center on a per-isotope basis due to lack of isotopic experimental data. Table IX gives computed worths and C/E values at each measurement position for the three plutonium sample traverses. Figures 10 through 12 illustrate the profiles in relation to the sample position in the core. The C/E values vary as a function of radial position. The uncertainties in the Pu-50 measurements in some cases overshadow the difference in the calculation and experiment. For all three samples the calculations show more spatial fine structure than the measurements near the outer-driver/radial-reflector boundary. This structure may have been lost due to streaming effects along the sample traverse tube.

Calculations of the reactivity worths of small composition changes near the center of the FTR can be improved by using the C/E values given in Tables VI and VII, provided similar analytical methods are used. Table IX and Figures 10 through 12 provide additional input for judging the reliability of calculated worths of small changes in plutonium isotopic composition in the outer core, radial reflector and near the core/reflector boundary. The uncertainties given in Tables VI, VII and IX are based on the statistical precision of the EMC measurements and should not be taken as 1σ accuracies for the quantities tabulated.

The largest discrepancies (greatest deviations from C/E = 1.0) observed in this analysis are for Fe_2O_3, stainless steel and ^{240}Pu. Poor cross section data is the most likely problem with ^{240}Pu. Future work should include

an assessment of the improvements that could be made by using some ENDF/B version IV cross section data and by an accurate determination of sample size and sample container effects.

7.0 ACKNOWLEDGMENTS

The authors wish to acknowledge the contribution to this report of personnel associated with the ZPR-9 critical facility at Argonne National Laboratory who performed the experiments described herein and transmitted the results to HEDL in the ANL-FFTF Informal Technical Progress Reports.

The authors would also like to express their appreciation to R. A. Bennett, R. B. Rothrock, R. W. Hardie, and J. V. Nelson for their comments and recommendations, to Nancy Petrowicz who assisted with the computations and tabulation of results, and to Mary Mudd and Betty Howard for their assistance in the preparation of the final draft of the report.

8.0 REFERENCES

1. K. D. Dobbin and J. W. Daughtry, Central Fuel Worth in the Fast Test Reactor (FTR) Engineering Mockup, HEDL-TME 75-52, Hanford Engineering Development Laboratory, Richland, WA, June 1975.

2. J. W. Daughtry and K. D. Dobbin, FFTF Test Loading Effects - Analysis of Experiments in the FTR Engineering Mockup Critical, HEDL-TME 76-34, Hanford Engineering Development Laboratory, Richland, WA, August 1976.

3. J. W. Daughtry and K. D. Dobbin, High ^{240}Pu Fuel Worth in the Fast Test Reactor Engineering Mockup, HEDL-TME 76-31, Hanford Engineering Development Laboratory, Richland, WA, May 1976.

4. K. D. Dobbin and J. W. Daughtry, Analysis of Control Rod Interaction Experiments in the FTR Engineering Mockup Critical, HEDL-TME 76-52, Hanford Engineering Development Laboratory, Richland, WA, March 1976.

5. J. W. Daughtry, Calculations of Eu_2O_3 and B_4C Worths in the Fast Test Reactor Engineering Mockup, HEDL-TME 75-34, Hanford Engineering Development Laboratory, Richland, WA, June 1975.

6. R. B. Kidman and R. E. Schenter, FTR Set 300S, Multigroup Cross Sections for FTR Shielding Calculations, HEDL-TME 71-184, Hanford Engineering Development Laboratory, Richland, WA, December 1971.

7. S. A. Cox, Delayed Neutron Data - Review and Evaluation, ANL/NDM-5, Argonne National Laboratory, Argonne, IL, April 1974.

8. J. W. Daughtry, "Delayed Neutron Parameters for the FFTF Engineering Mockup," in Core Engineering Technical Progress Report for July-September 1975, HEDL-TME 75-115, pp. 16-25, Hanford Engineering Development Laboratory, Richland, WA, December 1975.

9. J. W. Daughtry, C. D. Swanson, A. B. Long, R. B. Pond and G. K. Rusch, "ZPR-9 Assembly 27: The Fast Test Reactor Engineering Mockup Critical (FTR-EMC)," in Applied Physics Division Annual Report for July 1, 1970 to June 30, 1971, ANL-7910, pp. 32-39, Argonne National Laboratory, Argonne, IL, January 1972.

10. R. A. Bennett and P. L. Hofmann, Rationale and Plans for the FTR Critical Experiments Program, BNWL-490, Battelle Northwest Laboratory, Richland, WA, June 1967.

11. R. B. Pond, Reactor Physics Studies in the Engineering Mockup Critical Assembly of the Fast Test Reactor, ANL 76-42, Argonne National Laboratory, Argonne, IL, July, 1976.

12. R. J. Cornella, A. G. Long, and J. C. Beitel, "Small-Sample Measurements in the BOL-REF-5S Configuration of the FTR-EMC," in Reactor Development Program Progress Report for July 1974, ANL-RDP-30, pp. 6.6-6.15, Argonne National Laboratory, Argonne, IL, July 1974.

13. G. R. Keepin, Physics of Nuclear Kinetics, Addison-Wesley Publishing Company, Inc., Reading, MA, 1965.

14. R. E. Schenter, R. B. Kidman and J. V. Nelson, FTR Set 300, Multigroup Cross Sections for FTR Design, HEDL-TME 71-153, Hanford Engineering Development Laboratory, Richland, WA, October 1971.

15. R. E. Schenter, J. L. Baker and R. B. Kidman, ETOX, A Code to Calculate Group Constants for Nuclear Reactor Calculations, BNWL-1002, Battelle Northwest Laboratory, Richland, WA, May 1969.

16. R. M. Fleischman, Evaluation of the Modified Source Multiplication Technique for Subcritical Reactivity Assessments in FTR, HEDL-TME 74-53, Appendix A, Hanford Engineering Development Laboratory, Richland, WA, October 1974.

17. R. W. Hardie and W. W. Little, Jr., 3DB, A Three-Dimensional Diffusion Theory Burnup Code, BNWL-1264, Battelle Northwest Laboratory, Richland, WA, 1970.

18. R. W. Hardie and W. W. Little, Jr., 3DP, A Three-Dimensional Perturbation Theory Code, HEDL-TME 72-134, Hanford Engineering Development Laboratory, Richland, WA, December 1972.

19. R. M. Fleischman and J. V. Nelson, Three-Dimensional Neutronics Calculations for the Fast Test Reactor (FTR) and the FTR Engineering Mockup Critical Assembly (EMC), HEDL-TME 72-42, Hanford Engineering Development Laboratory, Richland, WA, April 1972.

20. D. R. Marr, A User's Manual for 2DBS, A Diffusion Theory Shielding Code, BNWL-1291, Battelle Northwest Laboratory, Richland, WA, February 1970.

21. R. W. Hardie and W. W. Little, Jr., PERT-V, A Two-Dimensional Perturbation Code for Fast Reactor Analysis, BNWL-1162, Battelle Northwest Laboratory, Richland, WA, September 1969.

22. R. W. Hardie, R. E. Schenter and R. E. Wilson, "An Analysis of Selected Fast Critical Assemblies Using ENDF/B-IV Neutron Cross Sections," in Nuclear Science and Engineering, Vol. 57, pp. 222-238, 1975.

23. J. W. Daughtry, R. B. Pond, C. D. Swanson and R. M. Fleischman, "ZPR-9 Assembly 26, FTR-3," in Applied Physics Division Annual Report for July 1, 1969 to June 30, 1970, ANL-7710, pp. 58-63, Argonne National Laboratory, Argonne, IL, January 1971.

24. S. Ramchandran and G. H. Madden, Analyses of FTR-3 Critical Experiments in Support of FTR Nuclear Design, WARD-2171-19, pp. 96-99, Westinghouse Advanced Reactors Division, Madison, PA, April 1971.

25. I. I. Bondarenko, et al., Group Constants for Nuclear Reactor Calculations, Consultants Bureau, New York, NY, 1964.

26. R. J. Tuttle, "Delayed-Neutron Data for Reactor Physics Analysis," Nuclear Science and Engineering, Vol. 56, pp. 37-71, January 1975.

27. P. J. Collins and R. G. Palmer, "Calculated Size Effects for Reactivity Samples in ZPPR," Transactions of the American Nuclear Society, Vol. 14, Number 2, p. 847, October 1971.